Autocorrelation Function and Power Spectrum of Two-State Random Processes Used in Neurite Guidance

David J. Odde* and Helen M. Buettner#

*Department of Chemical Engineering, Michigan Technological University, Houghton, Michigan 49931, and #Department of Chemical and Biochemical Engineering, Rutgers University, Piscataway, New Jersey 08855 USA

ABSTRACT During development neurons extend and retract cytoskeletal structures, chiefly microtubules and filopodia, to process informational cues from the extracellular environment and thereby guide growth cone migration toward an appropriate synaptic partner. This cytoskeleton-based exploration is achieved by stochastic switching, with microtubules and filopodia alternating between growing and shortening phases apparently at random. If stabilizing signals are not detected during the growth phase, then the structures switch to a shortening state, from which they can again return to a growth phase, and so forth. A useful means of characterizing these stochastic processes in a model-independent way is by autocorrelation and spectral analysis. Previously, we compared experiment to theory by performing Monte Carlo simulations and computing the autocorrelation function and power spectrum from the simulated dynamics, an approach that is computationally intensive and requires recalculation whenever model parameters are changed. Here we present analytical expressions for the autocorrelation function and power spectrum, which compactly characterize microtubule and filopodial dynamics based on the stochastic, two-state model. The model assumes that the phase times are of variable duration and gamma-distributed, consistent with experimental evidence for microtubules assembled in vitro from purified tubulin. The analytical expressions permit the precise quantitative characterization of changes in microtubule and filopodial searching behavior corresponding to changes in the shape of the gamma distribution.

INTRODUCTION

Neuronal growth is a highly dynamic and complex process that establishes specific synapses and ultimately results in a functional nervous system. To achieve this network of interconnections, neurons grow processes called neurites which have at their tips a highly motile structure referred to as the growth cone. The growth cone senses its environment and migrates in response to it in an attempt to locate an appropriate synaptic partner. This is partly accomplished by extending thin, actin-based protrusions called filopodia shown in Fig. 1 *A*. Filopodia extend for highly variable time periods and then retract if not stabilized by some positive interaction, for example by contacting specific guidepost cells during stereotypic pioneer axon extension (Bentley and Keshishian, 1982).

In a similar fashion microtubules grow and shorten, a phenomenon known as dynamic instability (Mitchison and Kirschner, 1984). The growth occurs by addition of the protein tubulin onto the distal microtubule tips. The transition to the shortening state is rapid and leads to extensive tubulin subunit loss from the microtubule lattice structure. The assembly of microtubules is critical for continued axonal growth since the application of microtubule destabilizing drugs results in growth cone collapse and neurite retraction (Yamada et al., 1970; Daniels, 1972; Bamburg et al., 1986). Typically, microtubules align parallel to each other in the axon but splay out in all directions in the growth cone, as shown in Fig. 1 *B*. Microtubules extend and retract via dynamic instability apparently in an attempt to locate regions of the growth cone periphery favorable for invasion by the remainder of the microtubule array. The invasion of microtubules into a particular region of the growth cone periphery leads to formation of the axon and growth cone advance (Sabry et al., 1991; Tanaka and Kirschner, 1991, 1995; Lin and Forscher, 1993). Based on this behavior, microtubules have been hypothesized to be important determinants of growth cone turning and reorientation (Tanaka and Kirschner, 1995).

For both microtubule and filopodial dynamics the key feature appears to be a rapid and stochastic switch between states of extension and retraction, idealized in Fig. 2, where *A* refers to extension and *B* to retraction. While the molecular mechanisms of these switches remain obscure, phenomenological models have been constructed to describe the observed dynamics of both microtubules (Hill, 1987; Mitchison and Kirschner, 1987; Bayley et al., 1989; Dogterom and Leibler, 1993; Gliksman et al., 1993; Odde and Buettner, 1995) and filopodia (Buettner et al., 1994). These models assume that microtubules and filopodia exist in either a growing or a shortening state with abrupt, random switches between states. The growth phases of microtubules (Odde et al., 1995) and filopodia (Buettner et al., 1994) are of highly variable duration and well-described by a gamma distribution, shown in Fig. 3 *A*, which has the probability density

$$f(t) = \frac{\nu^r t^{r-1} e^{-\nu t}}{\Gamma(r)} \tag{1}$$

Received for publication 29 July 1997 and in final form 13 June 1998.

Address reprint requests to Prof. David J. Odde, Department of Chemical Engineering, Michigan Technological University, Houghton, MI 49931. Tel.: 906-487-2140; Fax: 906-487-3213; E-mail: odde@mtu.edu.

© 1998 by the Biophysical Society

0006-3495/98/09/1189/08 $2.00

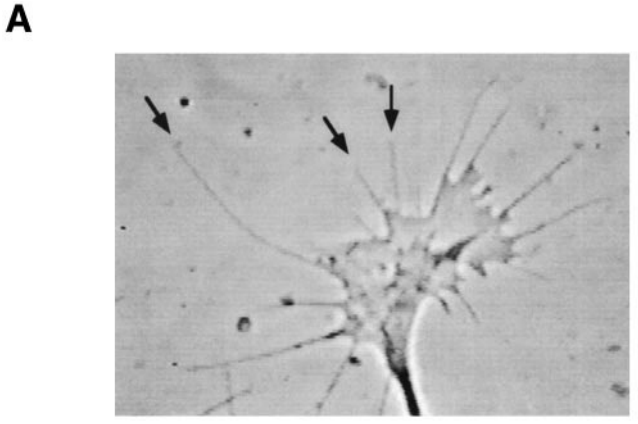

FIGURE 1 The nerve growth cone viewed by light microscopy. (*A*) Phase contrast image of an embryonic chick growth cone and its associated filopodia (three filopodia are marked by black arrows). (*B*) Fluorescent image of an embryonic frog growth cone and its microtubule array (courtesy of Drs. Elly Tanaka and Marc Kirschner, Harvard Medical School). Individual microtubules can be seen to extend well into the peripheral regions of the growth cone (marked by the three white arrows). Both microtubules and filopodia serve to guide the growth cone during normal development. Image widths are 85 μm (*A*) and 25 μm (*B*).

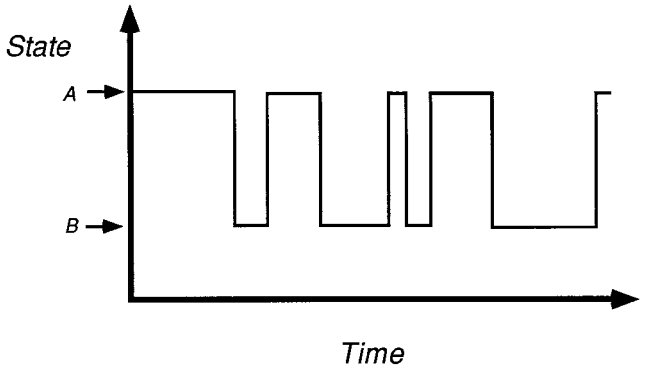

FIGURE 2 Idealized two-state behavior with stochastic switching. The amount of time spent in a given state before switching is highly variable and, in the present model, assumed to be gamma-distributed.

with parameters r and ν. When r is large the gamma distribution is symmetric and narrowly distributed about mean r/ν. At the other extreme, when $r = 1$, the distribution is exponential and broadly distributed. These parameters can be interpreted in terms of the kinetic scheme shown in Fig. 3 *B*: a series of r first-order events, each event occurring at rate ν, is required for a switch to occur. Typically, we have found r for microtubule and filopodial growth time distributions to be in the range $\sim$1–4 (Buettner et al., 1994; Odde and Buettner, 1995; Odde et al., 1995; Howell et al., 1997). In principle, the value of r for growth phases is independent of the value of r for shortening phases, although recent analysis demonstrated that the two values of r for microtubule dynamics in living cells are quite similar (Howell et al., 1997).

The similarity in microtubule and filopodial dynamics may be a direct reflection of a similarity in function: the growing structures sense their environment, integrate the signals received, and direct neuritic growth in response to the integrated information. The two-state model for process dynamics is useful in this respect since it permits a binary representation of the structure's state. For example, a microtubule in the growth state can be assigned the value "1," while a microtubule in the shortening state can be assigned the value "0," similar to the binary descriptors applied to represent gene expression (Kauffman, 1993). If this state is capable of switching in response to the local environment, then the microtubule can act as an information processor (Hameroff, 1987). This paradigm differs from the present view of cellular information processing where specific sets of signal transduction molecules (i.e., receptors, protein kinases, etc.) are responsible for intracellular signaling. A recent experiment supports the broader interpretation: when cultured fibroblasts are treated with microtubule depolymerizing agents, the transcriptional regulator, NF-κB, is specifically activated and associated genes expressed (Rosette and Karin, 1995). This result shows that a large number of microtubule switches from state 1 (growth) to state 0 (shortening) may result in a set of genes being changed from state 0 (not expressed) to state 1 (expressed).

In general, stochastic dynamics, such as those exhibited by microtubules and filopodia, can be conveniently characterized by the autocorrelation function and the power spectrum (Gardiner, 1985). The autocorrelation function characterizes the degree of correlation between values spaced τ time units apart while the power spectrum characterizes the degree of periodicity across a range of frequencies. Such analyses are especially useful because they characterize the system dynamics in a model-independent manner. For example, coevolving systems often "explore" their local environment via self-organized criticality (Bak et al., 1988; Kauffman, 1993). The autocorrelation and power spectrum can be used to characterize the experimentally measured dynamics of such a system and the results compared directly to model predictions. The power spectrum of microtubule dynamics in vitro was previously found to be consistent with the two-state model assuming gamma-distributed phase times, and exhibited power-law behavior consistent with a self-organized critical system (Odde et al., 1996a). In

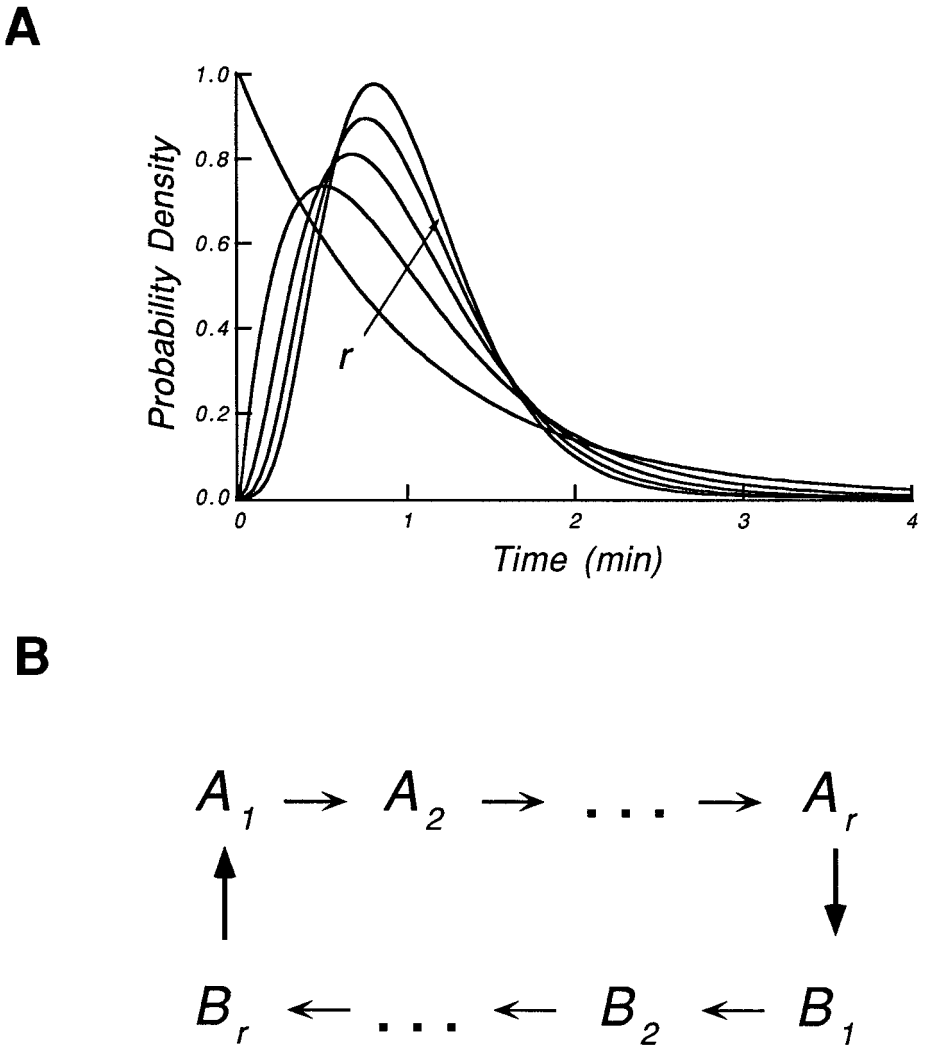

FIGURE 3 Gamma probability density and its associated kinetic model. (*A*) The gamma probability density is shown for values of $r = 1, 2, \ldots, 5$ (note that ν has been adjusted in each case to maintain a constant mean equal to 1 min). The distribution of phase times varies from an exponential decay when $r = 1$ to a more symmetric distribution when $r = 5$. (*B*) The associated kinetic model that gives rise to a gamma distribution of phase times. For a microtubule or filopodium to transit from state A_1 to state B_1, it must proceed through a series of $r - 1$ substates, $A_2, A_3, \ldots, A_r$, each step occurring at rate ν. A similar series of steps is then required for the reverse process. In principle the value of r for the growth phase (*A*) could be different from that for the shortening phase (*B*); however, the present analysis only considers the case where they are the same.

addition, microtubule dynamics in frog growth cones were found by autocorrelation analysis to be consistent with the two-state model having gamma-distributed phase times and displayed dynamics similar to those of the growth cone itself (Odde et al., 1996b). Thus, exploratory dynamics can generally be characterized by the autocorrelation function and power spectrum and directly compared to each other and to model predictions. However, this simulation-based approach is computationally intensive and requires that a new simulation be performed whenever a model parameter is changed.

To compactly describe the dynamics of filopodia and microtubules, we derived analytical expressions for the autocorrelation function and power spectrum of a two-state process with phase times that are gamma-distributed. For simplicity, we considered only integer values of the gamma distribution parameter, r (i.e., the special case given by the Erlang distribution). The analytical expressions provide precise quantitative characterization of microtubule and filopodial searching behaviors and their potential modulation during neurite outgrowth.

RESULTS

Analytical expressions for the autocorrelation function and power spectrum

Based on the two-state kinetic model shown in Fig. 3 *B*, we derived expressions for the autocorrelation function of microtubule and filopodial dynamics. The details of the derivation are given in the Appendix. For a two-state process with gamma-distributed phase times the autocorrelation function, $B(\tau)$, is given by

$$B(\tau) = \frac{1}{r}\left[\sum_{i=1}^{r}\sum_{j=0}^{r-i} P_j + \sum_{n=0}^{\infty}\sum_{i=1}^{r}\sum_{j=1}^{r}\left(P_{(2n+2)r-i+j} - P_{(2n+1)r-i+j}\right)\right] \quad (2)$$

where r is the gamma distribution shape parameter and

$$P_k = \frac{(\nu\tau)^k}{k!}e^{-\nu\tau} \quad (3)$$

where P_k is the probability (given by the Poisson distribution) of k first-order events occurring in a time interval τ,

each event occurring at rate ν. The power spectrum, $S(\omega)$, is directly related to the autocorrelation function by

$$S(\omega) = 2\int_0^\infty B(\tau)\cos\,\omega\tau\,d\tau \qquad (4)$$

where ω is the frequency.

Effect of varying *r*, the gamma distribution shape parameter

Previous analysis of growth time distributions suggested that the gamma distribution shape parameter, r, may represent a key parameter which the cell manipulates to effect changes in the state of the cytoskeleton (Odde et al., 1995). When r is varied across a range of values found experimentally for microtubules (Odde et al., 1995) and filopodia (Buettner et al., 1994), the autocorrelation function, $B(\tau)$, transits from a simple exponential decay for $r = 1$ to a damped oscillation for increasing values of r, the damping lessening with increasing r, as shown in Fig. 4 *A*. When $B(\tau) = 0$, there is no correlation between the present state and the state at a time τ later. Over long time intervals this is the case for finite values of r. The case where $B(\tau) = 1$ implies perfect correlation between states time τ apart. Thus, as $\tau \to 0$, $B(\tau) \to 1$, since the state is unlikely to change over very short time intervals. When $B(\tau) < 0$ there is anticorrelation to the present state, implying that if the system is in state A now it will tend to be in state B after a time τ from now. In the extreme where $B(\tau) = -1$, the

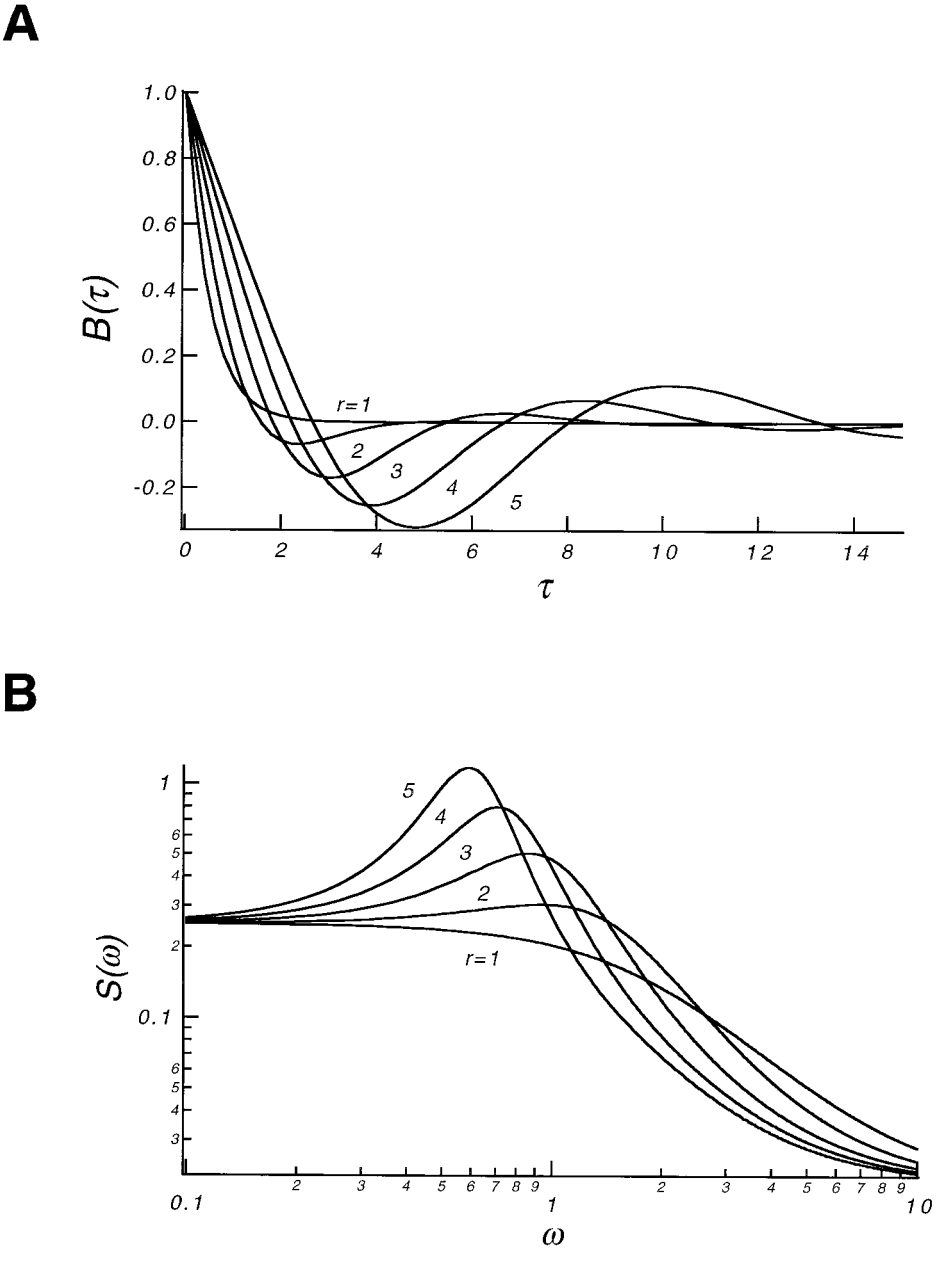

FIGURE 4 (*A*) Autocorrelation function and (*B*) power spectrum of a two-state process with gamma-distributed phase times. The gamma distribution shape parameter, r, is varied over the range $r = 1, 2, \ldots, 5$ (note that the parameter ν is held constant at 1). The autocorrelation function exhibits increased oscillations with increasing r while the power spectrum becomes more narrowly centered about the mean frequency, ω_{mean}.

system will always be in the opposite state after a time period τ has passed, which occurs for perfectly regular oscillations of frequency $\omega = \pi/\tau$, a limit that is approached as r becomes very large.

The power spectrum, $S(\omega)$, complements $B(\tau)$ by identifying the relative strength of various-sized oscillations in the process variable. The autocorrelation function and the power spectrum are not independent characterizations, however, since one is the Fourier transform of the other (Beckmann, 1968). We present both since each highlights different aspects of the stochastic process. The power spectrum, $S(\omega)$, is shown in Fig. 4 *B* as a function of the gamma distribution shape parameter, r. For the special case of $r = 1$, the power spectrum is distributed across a broad range of frequencies and is described by a Lorentzian of the form

$$S(\omega) = \frac{4\nu}{\omega^2 + 4\nu^2} \tag{7}$$

For increasing values of r the power spectrum becomes more narrowly centered about a mean cycle frequency defined as

$$\omega_{\text{mean}} \equiv \frac{\pi\nu}{r} \tag{8}$$

Thus, varying r can dramatically shift the effective range of frequencies that the two-state process exhibits.

DISCUSSION

Here we have presented analytical expressions for the autocorrelation function and power spectrum of a two-state process having gamma-distributed phase times. The analytical expressions provide compact descriptions of cytoskeletal dynamics so that computer simulation is not required to describe filopodial and microtubule exploratory behavior. The derived expressions for the autocorrelation function and power spectrum both show a strong dependence on r. The assumption of gamma-distributed phase times is necessary since the simple exponential distribution does not adequately account for the distributions observed experimentally for either microtubules or filopodia. Experimentally, it was previously estimated that $r \sim 3$ for microtubule growth times in vitro using purified tubulin to assemble the microtubules [6 μM tubulin, plus ends, axoneme fragments used as nucleating structures (Odde et al., 1995)]. Analysis of microtubule assembly data reported in the literature yielded values of r ranging from 1.4 to 4 across a range of conditions, both in vitro and in vivo (Odde and Buettner, 1995). In addition, microtubule phase times (both growing and shortening) in living newt lung epithelial cells exhibit gamma distributions having values of r within the range of the previously estimated values (Howell et al., 1997). Similarly, filopodia of chick dorsal root ganglia growth cones exhibit growth times that are gamma-distributed with a value of $r \sim 2$–3 (Buettner et al., 1994).

Given that r is generally not equal to 1, as has been previously assumed, it may be that r represents a key parameter modulated by the cell to effect a change in the state of the microtubule array. In support of this we have found that by simply changing r, and holding all other parameters constant, a cell can effect a change from an interphase-like microtubule array to a mitotic-like array (Odde et al., 1995). However, modulating r may not only provide a means of regulating the state of microtubules or filopodia, but also a means of optimizing the searching activity associated with these structures. The modulation of r could occur by any number of mechanisms. In the case of microtubules, the increasing tendency to switch the longer the microtubule has existed in the current state (as characterized by r) could simply be a result of the very slight increase in free energy of the microtubule polymer predicted (based on statistical mechanical arguments) to occur with increasing microtubule length (Hill, 1987). Thus, the observed gamma distribution could simply be a result of length-dependent switching between states A and B (Odde et al., 1995; Dogterom et al., 1996). Alternatively, the increasing tendency to switch could be a function not of microtubule length but rather of time spent in the current state, as originally proposed (Odde and Buettner, 1993, 1995). On the molecular level, this could be the result of the structural changes in tubulin subunits that occur at the microtubule tip during assembly and disassembly (Chretien et al., 1995). From the two reports of the phenomenon (Odde et al., 1995; Dogterom et al., 1996) it is not possible to discern which of these two possibilities is correct. Recent analysis of microtubule dynamics in newt cells seems to support the latter hypothesis: gamma-distributed phase times were observed ($r \sim 2$) even though microtubule length changes were typically $<\sim$10% of the total microtubule length. Further experimentation will be required to resolve this issue. The results of Howell et al. suggest that in either case the regulation of r is at least partially under the control of microtubule-associated proteins whose activity is in turn modulated by the phosphorylation state of the cell (Howell et al., 1997).

Stochastic searching activity and the gamma distribution

To illustrate how modulating the gamma shape parameter, r, can modulate the stochastic searching activity of microtubules and filopodia, we consider two extreme cases of the two-state model. The first is a two-state model with random, first-order transitions, which we call "random switching," and the second is a two-state model with perfectly regular transitions, which we call "regular switching." These two extremes can be represented within the context of the gamma distribution. If microtubules and filopodia are governed by *random switching*, then $r = 1$ and there will be a broad (exponential) distribution of phase times (see Fig. 3 *A*). Such microtubules and filopodia will undergo many

short extensions with occasional very long extensions. At the other extreme, *regular switching* occurs when all phase times are equal, which is the case when $r \rightarrow \infty$ (see Fig. 3 *A*). In this case, microtubules and filopodia will always undergo extensions of identical size.

The advantage of having $r = 1$, in terms of searching activity, is that a broad range of search sizes are attempted by the microtubules and filopodia. This strategy makes distant targets less likely to be missed, as can be seen from the right-hand tail of the gamma distribution shown in Fig. 3 *A*: a greater number of long times (relative to the mean time of 1 min) occur when $r = 1$ than for larger values of r. However, when $r = 1$ there is also a larger number of very short excursions relative to distributions having larger values of r. These short excursions presumably will contact an appropriate target only on rare occasions. Thus, the ability to locate distant targets comes at the expense of considerable energy expended on short, futile searches. The converse is true for the case when r is very large: while unable to contact distant targets, less energy is wasted on short searches. Here the energy spent by a microtubule or filopodium in searching its local environment is now entirely focused on searches of one particular size.

Based on these arguments, it would seem that the best strategy will depend greatly on the prior "knowledge" the searcher has about its local environment. Very often in the embryo, neurons develop in a very stereotypical and conserved manner (Jessell, 1991). In this case, r could evolve to a large value so that precise lengths of filopodia and microtubules are attained, lengths that exactly meet the requirements of the particular exploratory task. However, this strategy is very sensitive to small changes in the environment. If the target is moved a little further away than anticipated, the exploring structure cannot detect it since the structure is constrained to searches of one particular size. Thus, the greater r is the more fragile the searcher is, and the more susceptible it is to failure.

While the two-state model provides a useful model for characterizing microtubule and filopodial dynamics, deviations from the ideal behavior can occur. For instance, both microtubules (Schulze and Kirschner, 1986) and filopodia (Myers and Bastiani, 1993) have been observed to "pause" and neither grow nor shorten appreciably for a period of time. While nonideal, these dynamics are nevertheless readily amenable to autocorrelation and power spectrum analysis (Odde et al., 1996a; Vorobjev et al., 1997). The autocorrelation function and power spectrum can then be compared to the behavior predicted by various models, such as the two-state model. In addition, the analysis can be used to characterize the type of searching activity, whether more random (similar to when $r = 1$) or regular (similar to when r is large), independent of any particular model, two-state or otherwise. This approach is also useful when the underlying model is not known. For example, self-organized critical systems (Bak et al., 1988) and cooperative adsorption phenomena (Vlachos et al., 1991) can exhibit dynamics qualitatively similar to those of microtubules and filopodia. An interesting "higher-order" searching activity of the nervous system is the switching between visual perceptions of the Necker Cube, as shown in Fig. 5. The Necker Cube can elicit the perception of either of two solid cubes with stochastic switching between the two perceptions. Of particular interest to the present study is that the time spent in any one perception is gamma-distributed with a mode value of $r \sim 3$ [and varying between 1 and 9, depending on the subject (Borsellino et al., 1972)]. Therefore, the two-state process with gamma-distributed phase times may be a fundamental characteristic of stochastic exploration in biological and physical systems. Any putative searching activity ascribed to these systems can be quantitatively characterized by the autocorrelation function and power spectrum and comparison made to model prediction.

APPENDIX

Derivation of expressions for autocorrelation function and power spectrum

Consider a process that switches between two states, *A* and *B*, as idealized in Fig. 2. Furthermore, assume that r Poisson events (i.e., first-order reactions) in series are required for a switch to occur from state *A* to *B* and vice versa. The probability of k Poisson events occurring in a time interval τ is given by

$$P_{\mathrm{k}} = \frac{(\nu\tau)^{\mathrm{k}}}{k!} e^{-\nu\tau} \tag{A1}$$

where ν is the frequency of the Poisson events. To derive the expression for the autocorrelation function we consider each of the first r events and then calculate the probability of there being m switches during an arbitrary time interval τ. For example, assume that no Poisson events have occurred. If there are 0, 1, . . . , or $r - 1$ Poisson events, then there will be zero switches. If there are r, $r + 1$, . . . , or $2r - 1$ Poisson events, then there will be one switch. If there are $2r$, $2r + 1$, . . . , or $3r - 1$ Poisson events, then two switches will occur, and so forth. Next, assume that one Poisson event has occurred. If there are 0, 1, . . . , or $r - 2$ Poisson events, then there will be zero switches. If there are $r - 1$, r, . . . , or $2r - 2$ Poisson events, then

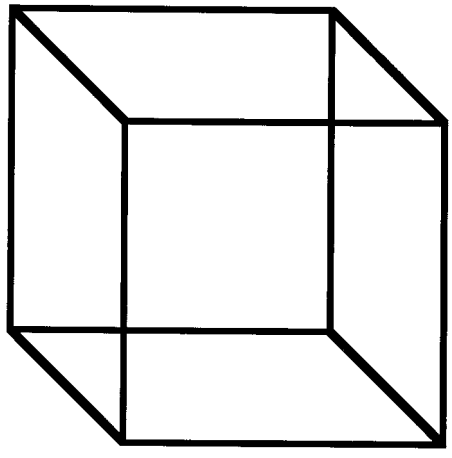

FIGURE 5 Necker Cube. Visual perception of a cube changes stochastically between either of two faces being closer. The distribution of times spent in any one perception has been shown previously to be gamma-distributed with a mode value for r of ~3.

there will be one switch. If there are $2r - 1$, $2r$, . . . , or $3r - 2$ Poisson events, then two switches will occur, and so forth. This procedure can be applied for each of the first r intervals.

We can now calculate the probability of 0, 1, 2, or more switches occurring by adding all the probabilities together. For example, the probability of zero switches is given by

$$\text{prob}[m = 0 \text{ in interval } (t, t + \tau)] = \frac{1}{r}[(P_0 + P_1 + \cdots + P_{r-1}) + (P_0 + P_1 + \cdots + P_{r-2}) + \cdots + P_0] \quad \text{(A2)}$$

or

$$\text{prob}[m = 0 \text{ in interval } (t, t + \tau)] = \frac{1}{r}\sum_{i=0}^{r}\sum_{j=0}^{r-i} P_j \quad \text{(A3)}$$

Similarly, the probability of one switch is given by

$$\text{prob}[m = 1 \text{ in interval } (t, t + \tau)] = \frac{1}{r}[(P_r + P_{r+1} + \cdots + P_{2r-1}) + (P_{r-1} + P_r + \cdots + P_{2r-2}) + \cdots + (P_1 + P_2 + \cdots + P_r)] \quad \text{(A4)}$$

or

$$\text{prob}[m = 1 \text{ in interval } (t, t + \tau)] = \frac{1}{r}\sum_{i=1}^{r}\sum_{j=1}^{r} P_{(r-i)+j} \quad \text{(A5)}$$

In general, for $m > 0$, the probability of m switches occurring is given by

$$\text{prob}[m, m \text{ integer} > 0, \text{ in interval } (t, t + \tau)] = \frac{1}{r}\sum_{i=1}^{r}\sum_{j=1}^{r} P_{rm-i+j} \quad \text{(A6)}$$

From these probabilities the autocorrelation function can be derived. If there are an even number of m switches during time $t + \tau$, the state will be the same as it was at time t. Alternatively, if there are an odd number of switches, then the state at time $t + \tau$ will be the opposite of the original state at time t. For an even number of switches, the probability is given by

$$\text{prob}(m \text{ even}) = \frac{1}{r}\sum_{i=0}^{r}\sum_{j=0}^{r-i} P_j + \frac{1}{r}\sum_{n=0}^{\infty}\sum_{i=1}^{r}\sum_{j=1}^{r} P_{(2n+2)r-i+j} \quad \text{(A7)}$$

and for an odd number of switches the probability is given by

$$\text{prob}(m \text{ odd}) = \frac{1}{r}\sum_{n=0}^{\infty}\sum_{i=1}^{r}\sum_{j=1}^{r} P_{(2n+1)r-i+j} \quad \text{(A8)}$$

The autocorrelation function, $B(\tau)$, is then given by

$$B(\tau) = \text{prob}(m \text{ even}) - \text{prob}(m \text{ odd}) \quad \text{(A9)}$$

Combining Eqs. A7–A9, we arrive at the final expression for $B(\tau)$, which is given by

$$B(\tau) = \frac{1}{r}\left[\sum_{i=1}^{r}\sum_{j=0}^{r-i} P_j + \sum_{n=0}^{\infty}\sum_{i=1}^{r}\sum_{j=1}^{r}(P_{(2n+2)r-i+j} - P_{(2n+1)r-i+j})\right] \quad \text{(A10)}$$

Since the autocorrelation function and power spectrum are Fourier transforms of each other (Beckmann, 1968), we can obtain the power spectrum, $S(\omega)$, from Eq. A10. The expression for the power spectrum, $S(\omega)$, is therefore given by

$$S(\omega) = 2\int_0^{\infty} B(\tau)\cos\,\omega\tau\,d\tau \quad \text{(A11)}$$

The authors thank Dr. Nader Moayeri for helpful discussions and comments. This work was supported by National Science Foundation Grant BCS 92-10540.

REFERENCES

Bak, P., C. Tang, and K. Wiesenfeld. 1988. Self-organized criticality. *Phys. Rev. A.* 38:364–374.

Bamburg, J. R., D. Bray, and K. Chapman. 1986. Assembly of microtubules at the tip of growing axons. *Nature.* 321:788–790.

Bayley, P. M., M. J. Schilstra, and S. R. Martin. 1989. A simple formulation of microtubule dynamics: quantitative implications of the dynamic instability of microtubule populations in vivo and in vitro. *J. Cell Sci.* 93:241–254.

Beckmann, P. 1968. Elements of Applied Probability Theory. Harcourt, Brace & World, New York.

Bentley, D., and H. Keshishian. 1982. Pathfinding by peripheral pioneer neurons in grasshoppers. *Science.* 218:1082–1088.

Borsellino, A., A. De Marco, A. Allazetta, S. Rinesi, and B. Bartolini. 1972. Reversal time distribution in the perception of visual ambiguous stimuli. *Kybernetik.* 10:139–144.

Buettner, H. M., R. Pittman, and J. Ivins. 1994. A model of neurite extension across regions of nonpermissive substrate: simulations based on experimental measurement of growth cone motility and filopodia dynamics. *Dev. Biol.* 163:407–422.

Chretien, D., S. D. Fuller, and E. Karsenti. 1995. Structure of growing microtubule ends: two-dimensional sheets close into tubes at variable rates. *J. Cell Biol.* 129:1311–1328.

Daniels, M. P. 1972. Colchicine inhibition of nerve fiber formation in vitro. *J. Cell Biol.* 53:164–176.

Dogterom, M., M.-A. Felix, C. C. Guet, and S. Leibler. 1996. Influence of M-phase chromatin on the anisotropy of microtubule asters. *J. Cell Biol.* 133:125–140.

Dogterom, M., and S. Leibler. 1993. Physical aspects of the growth and regulation of microtubule structures. *Phys. Rev. Lett.* 70:1347–1350.

Gardiner, C. W. 1985. Handbook of Stochastic Methods for Physics, Chemistry, and the Natural Sciences, 2nd ed. Springer-Verlag, Berlin.

Gliksman, N. R., R. V. Skibbens, and E. D. Salmon. 1993. How the transition frequencies of microtubule dynamic instability (nucleation, catastrophe, and rescue) regulate microtubule dynamics in interphase and mitosis: analysis using a Monte Carlo computer simulation. *Mol. Biol. Cell.* 4:1035–1050.

Hameroff, S. R. 1987. Ultimate Computing. Elsevier, Amsterdam.

Hill, T. L. 1987. Linear Aggregation Theory in Cell Biology. Springer-Verlag, New York.

Howell, B., D. J. Odde, and L. Cassimeris. 1997. Kinase and phosphatase inhibitors cause rapid alterations in microtubule dynamic instability in living cells. *Cell Motil. Cytoskel.* 38:201–214.

Jessell, T. M. 1991. Cell migration and axon guidance. *In* Principles of Neural Science. E. R. Kandel, J. H. Schwartz, and T. M. Jessell, editors. Elsevier Science Publishing, New York. 908–928.

Kauffman, S. A. 1993. The Origins of Order. Oxford University Press, New York.

Lin, C.-H., and P. Forscher. 1993. Cytoskeletal remodeling during growth cone-target interactions. *J. Cell Biol.* 121:1369–1383.

Mitchison, T. J., and M. W. Kirschner. 1984. Dynamic instability of microtubule growth. *Nature.* 312:237–242.

Mitchison, T. J., and M. W. Kirschner. 1987. Some thoughts on the partitioning of tubulin between monomer and polymer under conditions of dynamic instability. *Cell Biophys.* 11:35–55.

Myers, P. Z., and M. J. Bastiani. 1993. Growth cone dynamics during the migration of an identified commissural growth cone. *J. Neurosci.* 13: 127–143.

Odde, D. J., and H. M. Buettner. 1993. A time series approach to characterizing microtubule dynamics. *Mol. Biol. Cell.* 4:164*a*. (Abstr.).

Odde, D. J., and H. M. Buettner. 1995. Time series characterization of simulated microtubule dynamics in the nerve growth cone. *Ann. Biomed. Eng.* 23:268–286.

Odde, D. J., L. Cassimeris, and H. M. Buettner. 1995. Kinetics of microtubule catastrophe assessed by probabilistic analysis. *Biophys. J.* 69: 796–802.

Odde, D. J., L. Cassimeris, and H. M. Buettner. 1996a. Spectral analysis of microtubule assembly dynamics. *AIChE J.* 42:1434–1442.

Odde, D. J., E. M. Tanaka, S. S. Hawkins, and H. M. Buettner. 1996b. Stochastic dynamics of the nerve growth cone and its microtubules during neurite outgrowth. *Biotechnol. Bioeng.* 50:452–461.

Rosette, C., and M. Karin. 1995. Cytoskeletal control of gene expression: depolymerization of microtubules activates NF-κB. *J. Cell Biol.* 128: 1111–1119.

Sabry, J. H., T. P. O'Connor, L. Evans, A. Toroian-Raymond, M. Kirschner, and D. Bentley. 1991. Microtubule behavior during guidance of pioneer neuron growth cones in situ. *J. Cell Biol.* 115:381–395.

Schulze, E., and M. Kirschner. 1986. Microtubule dynamics in interphase cells. *J. Cell Biol.* 102:1020–1031.

Tanaka, E., and M. W. Kirschner. 1995. The role of microtubules in growth cone turning at substrate boundaries. *J. Cell Biol.* 128:127–137.

Tanaka, E. M., and M. W. Kirschner. 1991. Microtubule behavior in the growth cones of living neurons during axon elongation. *J. Cell Biol.* 115:345–363.

Vlachos, D. G., L. D. Schmidt, and R. Aris. 1991. Bifurcations and global stability in surface catalyzed reactions using the Monte Carlo method. *In* Patterns and Dynamics in Reactive Media. R. Aris, D. G. Aronson, and H. L. Swinney, editors. Springer-Verlag, New York. 187–206.

Vorobjev, I. A., T. M. Svitkina, and G. G. Borisy. 1997. Cytoplasmic assembly of microtubules in cultured cells. *J. Cell Sci.* 110:2635–2645.

Yamada, K. M., B. S. Spooner, and N. K. Wessells. 1970. Axon growth: roles of microfilaments and microtubules. *Proc. Natl. Acad. Sci. USA.* 66:1206–1212.